Int. J. Heat Mass Transfer. Vol. 28, No. 8, pp. 1575–1586, 1985
Printed in Great Britain

0017–9310/85 $3.00 + 0.00
Pergamon Press Ltd.

Design theory for rotary heat and mass exchangers—I. Wave analysis of rotary heat and mass exchangers with infinite transfer coefficients

E. VAN DEN BULCK, J. W. MITCHELL and S. A. KLEIN

Solar Energy Laboratory, University of Wisconsin–Madison, 1500 Johnson Drive, Madison, WI 53706, U.S.A.

(*Received* 31 *August* 1984 *and in final form* 4 *February* 1985)

Abstract—A theory is presented for modeling rotary heat and mass exchangers with infinite transfer coefficients. The continuity and energy conservation equations for one-dimensional transient flow are established and analyzed. Solutions to the equations are obtained by the method of characteristics and the shock wave method. Both methods provide a set of analytical equations that allow performance prediction of the heat and mass exchanger with infinite transfer coefficients for any inlet and operating conditions. A regenerator-operating chart is introduced which shows the fundamental modes of operation for rotary heat and mass exchangers. Part II presents correlations for the effectiveness of rotary dehumidifiers with finite transfer coefficients.

1. INTRODUCTION

ROTARY heat and mass exchangers are currently employed in desiccant cooling and drying systems. Desiccant systems may be applied in a variety of industrial processes that require cool and dry air. These processes include drying of powders and wood [1], production, processing and storage of chemicals and food [2], and humidity control of warehouses and computer rooms [3]. Desiccant systems may also be used for air-conditioning of living and working spaces [4–9]. In these systems, air is dried by passing it over a desiccant and subsequently through a heat exchanger in which the heat of sorption is removed by sensible cooling. This processed air may be further cooled by adiabatic humidification to yield a dry and cool air stream [10]. Thermal energy is used to regenerate the desiccant. The use of solar energy as source for regeneration heat offers an opportunity for energy conservation in industrial [1–3] and residential [4–10] energy use.

Silica gel [4–8] and molecular sieves [9] are the desiccants presently under investigation for air-conditioning purposes. The dehumidifier may be arranged as a cross-flow adiabatic [4] or cooled [5] matrix, as a packed bed rotating drum [6], or as a rotating wheel with axial counterflow of both air streams [7–9]. The design showing the best prospects is the rotary counterflow conception, which combines high performance with compactness.

Rotary dehumidifiers have been modeled by equations expressing the conservation of mass and energy, and rates of transfer of heat and mass. For various simplifying assumptions, these equations have been solved analytically and numerically. Banks [11] and Close and Banks [12] have introduced the analogy theory which was developed to model sorbent bed performance and later was applied to predict regnerator performance [13–15]. In this theory, the temperature and humidity ratio of the moist air stream are combined into two independent potentials. When the conservation equations for mass and energy are expressed in terms of these potentials, they become analogous to the energy equation for thermal regenerators. Dehumidifier performance may then be calculated using existing regenerator performance correlations [16]. Mathiprakasam and Lavan [17] have presented an analytical model for cross-flow and rotating adiabatic dehumidifiers. In their solution method, the conservation and rate equations are first linearized and then solved using Laplace transforms. Because of the simplifications needed to perform the analysis, the analogy theory and linear solution method are limited to regenerators with equal overall transfer coefficients for heat and mass (i.e. Lewis number equal to one).

Several codes [14, 18, 19] exist that model the dehumidifier by solving the conservation and transfer rate equations by means of a finite-difference method. The matrix is divided into a two-dimensional time–space grid, and changes in enthalpy and humidity of the desiccant and the air stream when passing through a grid element are calculated using various approximations. These codes agree well with experimental data of dehumidifier performance [20]. However, finite-difference programs involve considerable computation and are not suited for long-term simulation of desiccant cooling systems.

For a given pair of inlet states, dehumidifier performance is determined by the operating conditions (i.e. mass of desiccant, wheel speed and air stream flow rates) and transfer coefficients. The effect of operating conditions on the outlet states of the dehumidifier may be studied by looking first at regenerators with infinite

NOMENCLATURE

a_i	auxiliary state property functions
A_j	total heat transfer area of the dehumidifier matrix in period j [area]
c_p	moist air specific heat [energy/(dry-mass–temperature)]
F_i	ith combined heat and mass potential [dimensions arbitrary]
h_t	heat transfer coefficient [energy/(area–time–temperature)]
h_w	mass transfer coefficient [mass/(area–time)]
i	moist air enthalpy [energy/dry mass]
i_v	water vapor enthalpy [energy/mass]
I	matrix enthalpy [energy/dry mass]
L	axial flow length through the matrix [length]
$\dot{m}$	mass flow rate [mass/time]
M_d	mass of desiccant in the dehumidifier matrix [mass]
M_f	mass of air in the dehumidifier matrix [mass]
NTU_t	number of transfer units for heat transfer, $h_t A/\dot{m}c_p$ [dimensionless]
NTU_w	number of transfer units for mass transfer, $h_w A/\dot{m}$ [dimensionless]
S_i	ith shock wave speed [dimensionless]
t	temperature
T	time required for a complete rotation of the matrix [time]
w	moist air humidity rate [dimensionless]
W	matrix water content [dimensionless]
x	axial coordinate measured from period entrance [dimensionless]
z	axial displacement through matrix measured from period entrance [length].

Greek symbols

Γ_j	jth capacitance rate parameter of the rotary dehumidifier [dimensionless]
θ	time
θ_j	duration of period j [time]
λ_i	ith characteristic wave speed [dimensionless]
τ	time coordinate [dimensionless]
τ_{dj}	dwell time of a fluid particle in period j [time].

Subscripts

d	desiccant
f	evaluated at fluid state
i	combined potential index
int	evaluated at intersection point of F_1 characteristic through the period 1 inlet state and the F_2 characteristic through the period 2 inlet state
j	period index
m	evaluated at, or in equilibrium with, the matrix state
P	processing
R	regeneration
s	evaluated at shock state
t	heat transfer or temperature
w	mass transfer or moisture.

Superscripts

$\cdot$	rate
$\bar{}$	average value for a period.

transfer coefficients. Secondly, the effect of transfer parameters may be described in terms of an effectiveness, in which the actual dehumidifier is compared to the ideal dehumidifier. This approach leads to the formulation of an Effectiveness–Number of Transfer Units (NTU) method for rotary heat and mass exchangers, which is presented in this paper. The ε–NTU approach clearly shows the separate effects of flow unbalance and transfer coefficients, as opposed to existing methods [13, 17] that solve the conservation and rate of transfer equations simultaneously.

Part I of this paper presents an analysis of solid desiccant ideal rotary dehumidifiers. The conservation equations for mass and energy are solved by means of a wave analysis. Equations are provided to calculate ideal dehumidifier outlet states as functions of the inlet states and two dimensionless capacitance rate parameters. A dehumidifier operating chart is introduced that shows the fundamental modes of operation for rotary heat and mass exchangers. Part II presents expressions for the humidity and enthalpy effectiveness for silica gel dehumidifiers as functions of the dehumidifier NTU. The correlations for effectiveness and ideal dehumidifier performance yield rapid prediction of the actual dehumidifier performance.

2. MODEL FORMULATION AND ASSUMPTIONS

The nomenclature and coordinate system for the rotary dehumidifier are illustrated in Fig. 1. The adsorbent matrix is arranged as a rotating cylindrical wheel of length L and has a total mass of dry desiccant M_d. Two air streams are blown in counterflow through the regenerator. The process air stream has a low temperature and high relative humidity while the regeneration air stream has a high temperature and low

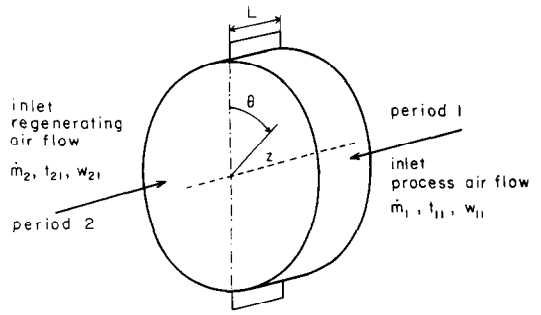

FIG. 1. Nomenclature and coordinate system for the rotary heat and mass exchanger.

relative humidity. For each period, the axial coordinate, z, is defined as positive in the fluid flow direction, while the rotary position is indicated by the time coordinate θ.

The model which describes the exchange of heat and mass between the moist air and the desiccant matrix is based on the following conventional assumptions for this situation [11, 14]:

(1) The matrix is modeled as being of parallel passage form, consisting of a homogeneous solid with constant matrix characteristics and porosity, through which an air–water vapor mixture flows with constant velocity. Pressure drop effects through the bed are small with respect to absolute pressure [6], and are neglected.
(2) The state properties of the air streams are spatially uniform at the inlet of each period. There is no mixing or carry-over of streams.
(3) A transient one-dimensional approach is applied. There is no radial variation of fluid or matrix states, and diffusion fluxes of heat and mass due to tangential gradients of matrix and air state properties are neglected.
(4) The axial heat conduction and water vapor diffusion flux are negligible in both the matrix and air streams.
(5) The thermal and moisture capacities of the air entrained in the matrix are negligible compared to the matrix capacities.
(6) Transport of water vapor through the air occurs only through ordinary diffusion and transport of heat occurs only through ordinary heat conduction. Flux coupling is neglected.
(7) The heat and mass transfer processes between the desiccant matrix and the air stream can be described by lumped transfer coefficients.
(8) The periodic steady-state performance of the dehumidifier is considered.

The capacitance rate parameters, Γ_1 and Γ_2, are defined as the ratio of matrix mass to fluid mass capacity rate:

$$\Gamma_j = \frac{M_{dj}\tau_{dj}}{\theta_j M_{fj}} = \frac{M_d}{T\dot{m}_j}; \quad j = 1, 2 \tag{1}$$

and the following dimensionless coordinates are introduced:

$$x = \frac{z}{L}; \quad 0 \leqslant x \leqslant 1$$
$$\tau = \frac{\theta}{\tau_{dj}}\frac{M_{fj}}{M_{dj}} = \frac{\theta}{\theta_j}\frac{1}{\Gamma_j}; \quad 0 \leqslant \tau \leqslant \frac{1}{\Gamma_j}. \tag{2}$$

Under assumptions 1–8, the conservation and transfer rate equations for period j of the heat and mass regenerator have been written as [13]:

$$\frac{\partial w_f}{\partial x} + \frac{\partial W_m}{\partial \tau} = 0$$

$$\frac{\partial w_f}{\partial x} = NTU_{w,j}(w_m - w_f)$$

$$\frac{\partial i_f}{\partial x} + \frac{\partial I_m}{\partial \tau} = 0$$

$$\frac{\partial i_f}{\partial x} = NTU_{t,j}\frac{\partial i_f}{\partial t_f}(t_m - t_f) + i_v NTU_{w,j}(w_m - w_f) \tag{3}$$

$NTU_{t,j}$ and $NTU_{w,j}$ are the number of transfer units for heat and mass, respectively, and are defined as conventional.

Equations (3) are coupled through the thermodynamic property relationships for the desiccant–air–water vapor mixture. Property relations for desiccants may be obtained from the literature [21] and presented in the functional form indicated in equation (4):

$$i_f = i_f(w_f, t_f)$$
$$I_m = I_m(W_m, t_m)$$
$$w_m = w_m(W_m, t_m). \tag{4}$$

The initial conditions for this system of equations are:

for

$$0 \leqslant \tau \leqslant \frac{1}{\Gamma_j}; \quad w_f(x = 0, \tau) = w_{j1}$$
$$i_f(x = 0, \tau) = i_{j1}, \quad j = 1, 2. \tag{5}$$

The periodic equilibrium boundary conditions for the matrix state properties are:

for $0 \leqslant x \leqslant 1$;

$$\lim_{\tau_1 \to (1/\Gamma_1)^-} [W_m(x, \tau_1)] = \lim_{\tau_2 \to 0^+} [W_m(1-x, \tau_2)]$$

$$\lim_{\tau_1 \to (1/\Gamma_1)^-} [I_m(x, \tau_1)] = \lim_{\tau_2 \to 0^+} [I_m(1-x, \tau_2)]$$

$$\lim_{\tau_1 \to 0^+} [W_m(x, \tau_1)] = \lim_{\tau_2 \to (1/\Gamma_2)^-} [W_m(1-x, \tau_2)]$$

$$\lim_{\tau_1 \to 0^+} [I_m(x, \tau_1)] = \lim_{\tau_2 \to (1/\Gamma_2)^-} [I_m(1-x, \tau_2)]. \tag{6}$$

In the ideal dehumidifier, the overall heat and mass transfer coefficients are infinite. Thus at all times, each differential desiccant–moist air subsystem is in

complete thermodynamic equilibrium (i.e. thermal and vapor pressure equilibrium). The conservation equations (3) then reduce to

$$\frac{\partial w_m}{\partial x} + \frac{\partial W_m}{\partial \tau} = 0$$
$$\frac{\partial i_m}{\partial x} + \frac{\partial I_m}{\partial \tau} = 0. \quad (7)$$

Equations (7) combined with the property relationships (4) and the initial and boundary conditions (5), (6), form a system of two coupled conservation laws. Each is a hyperbolic partial differential equation, and is nonlinear because of the nonlinear property relationships. Solutions may be obtained by the method of characteristics [22, 23] and the shock wave method [23]. This approach is applied in the following analysis.

3. WAVE ANALYSIS OF THE CONSERVATION EQUATIONS

Following Lax [22], the two-dimensional hyperbolic system of conservation laws (7) has two characteristics which are defined by the following ordinary differential equation:

$$\frac{dx}{d\tau} = \lambda_i; \quad i = 1, 2. \quad (8a)$$

The speeds λ_i are given by the roots of the equation of direction of the characteristics [23]:

$$a_1 a_5 \lambda - (a_2 - \lambda)(a_3 \lambda - a_4) = 0. \quad (8b)$$

In this expression, the state property functions $a_i(t_m, w_m)$ are defined as

$$a_1(t_m, W_m) = \left(\frac{\partial w_m}{\partial t_m}\right)_{W_m}$$
$$a_2(t_m, W_m) = \left(\frac{\partial w_m}{\partial W_m}\right)_{t_m}$$
$$a_3(t_m, W_m) = \left(\frac{\partial I_m}{\partial t_m}\right)_{W_m}$$
$$a_4(t_m, W_m) = \left(\frac{\partial i_m}{\partial t_m}\right)_{w_m}$$
$$a_5(t_m, W_m) = \left(\frac{\partial I_m}{\partial W_m}\right)_{t_m} - \left(\frac{\partial i_m}{\partial w_m}\right)_{t_m} \quad (8c)$$

and may be obtained from the state property correlations (4). Along the characteristics, the state properties of the fluid stream satisfy the equation

$$(a_1 a_3)\, dt_m + (a_1 a_5 + a_3 \lambda_i - a_4)\, dW_m = 0; \quad i = 1, 2. \quad (8d)$$

Integration of expression (8d) along the characteristic (8a) yields

$$dF_i = 0; \quad i = 1, 2. \quad (8e)$$

The functions F_i are the Riemann invariants of the system of equations (7). They were first introduced for desiccant systems by Banks *et al.* [11–13] and were named the F_i potentials because they are state property functions of the desiccant–fluid system. For each system defined by the equilibrium property relationships (4), the F_i potentials may be obtained through numerical integration of equation (8d). Maclaine-cross [14] has developed F_1-F_2 charts for the systems air–water vapor with calcium chloride, lithium chloride and lithium bromide as the desiccant. Jurinak [15, 21] has developed analytical curve fits for the F_i potentials in terms of air temperature and humidity ratio for the system: silica gel–air–water vapor. His expressions may be rewritten as

$$F_1 = 10.0 + 12.0\left[\frac{2865.0}{(t_m + 273.0)^{1.490}} + 4.244 w_m^{0.8624}\right] \quad (9)$$

$$F_2 = 3.0 + 12.0\left[\frac{(t_m + 273.0)^{1.490}}{6360.0} - 1.127 w_m^{0.07969}\right]$$

where the units of t_m and w_m are °C and kg kg^{-1}, respectively. For silica gel, lines of constant F_1 resemble lines of constant enthalpy in a psychrometric chart, whereas lines of constant F_2 resemble lines of constant relative humiditity. Figure 2 illustrates an F_1-F_2 chart with lines of constant temperature and air humidity. If F_1 is constant, the temperature increases as the humidity decreases. For constant F_2, the temperature increases with humidity.

Maclaine-cross [13, 14] and Banks [13, 15] use the concept of F_i potentials to predict the performance of rotary dehumidifiers with finite transfer coefficients. Their technique is based upon the analogy between the characteristic expressions (8d) that model heat and mass exchangers and the expressions that model regenerators with heat transfer alone [16]. In this paper, the wave analysis is completed to include shock waves and to model exactly dehumidifers with infinite transfer coefficients.

The F_i potential is constant along the λ_i characteristic. Thus, values of constant F_i propagate

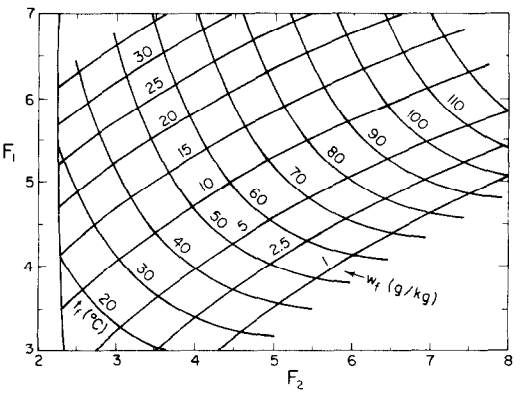

FIG. 2. Air temperature and humidity ratio in an F_1-F_2 chart for moist air–silica gel.

through the matrix at speed λ_i and this process may be interpreted as a state property wave moving with speed λ_i. This wave speed is a local speed and depends only upon the local state properties at the point of interest. Lines of constant λ_1 are shown in an F_1-F_2 chart in Fig. 3, and λ_2-lines are shown in Fig. 4. λ_1 is the speed at which the F_1 potential moves through the desiccant bed, while λ_2 is the corresponding speed for the F_2 potential. For moist air–silica gel, λ_1 is about 10–100 times larger than λ_2 and both are positive. Thus, the F_1 wave propagates much faster through the desiccant matrix than the wave carrying the F_2 invariant and both waves move in the direction of the air stream flow. Figure 3 shows that λ_1 increases with F_1 for constant F_2, and Fig. 4 shows that λ_2 increases with F_2 for constant F_1. Expansion waves or shock waves will therefore occur depending on the initial value problem associated with the system of conservation equations (7).

The following ranges for process and regeneration air inlet states are typical for well-defined desiccant dehumidification systems [21]:

$$t_{11} \leqslant 35.0°C$$
$$w_{11} \leqslant 20.0\ \text{g kg}^{-1}$$
$$t_{21} \geqslant 60.0°C$$
$$w_{21} \geqslant 10.0\ \text{g kg}^{-1}. \qquad (10a)$$

For these inlet conditions, Fig. 2 shows that the following relationships hold for the F_i potentials:

$$F_{1,11} \leqslant F_{1,21}$$
$$F_{2,11} \leqslant F_{2,21}. \qquad (10b)$$

The F_i potentials of the process air inlet state are smaller than the F_i potentials associated with the regeneration air inlet state.

Figure 5(a) illustrates the initial value problem associated with the flow of the process air stream over a desiccant, which is initially in equilibrium with the regeneration air inlet state. The leading edge of the F_i distribution carries the high F_i potential associated with the initial state. The trailing edge is at the low value

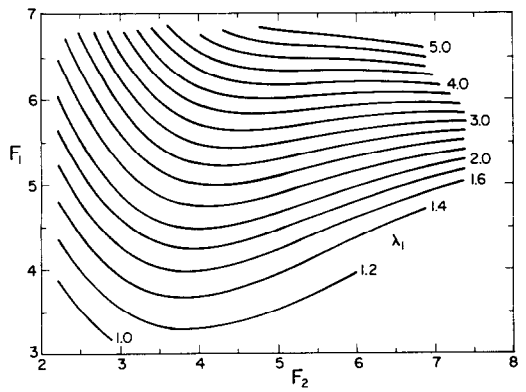

FIG. 3. Wave speed λ_1 in an F_1-F_2 chart for moist air–silica gel.

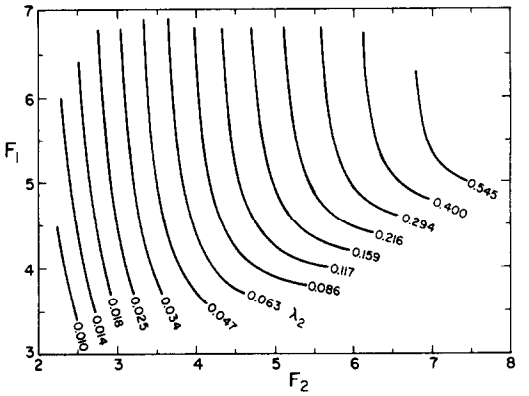

FIG. 4. Wave speed λ_2 in an F_1-F_2 chart for moist air–silica gel.

of the incoming process stream. Since the high potential propagates through the matrix at a higher speed than the low potential, the F_1 and F_2 waves spread out as time proceeds. Two separated rarefaction waves are generated during the dehumidification of the process air stream. The state after passage of the tail of the F_1 wave and before arrival of the edge of the F_2 wave has been defined [13–15] as the intersection point state. The intersection point state has the F_1 potential of the incoming process air stream and the F_2 potential of the initial state:

$$F_{1,\text{int}}(t_{\text{int}}, w_{\text{int}}) = F_{1,11}$$
$$F_{2,\text{int}}(t_{\text{int}}, w_{\text{int}}) = F_{2,21}. \qquad (11)$$

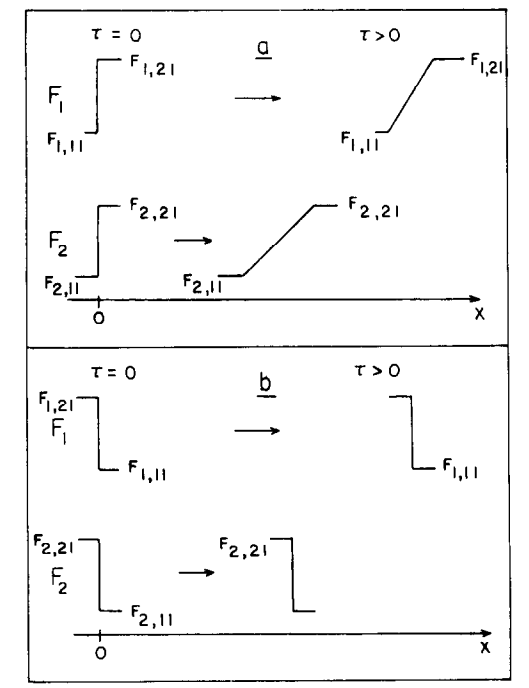

FIG. 5. Initial value problems associated with processing (a) and regenerating (b) a desiccant matrix.

This set of two nonlinear equations in two unknowns may be solved numerically [e.g. using equations (9)] to yield the intersection point state (t_{int}, w_{int}).

Figure 5(b) illustrates the alternate problem. Regeneration air is passed over the desiccant that is initially in equilibrium with the process air inlet state. The F_i distributions are initially square with the tail of each wave carrying the respective high potential of the incoming regeneration air. This tail has the tendency to move faster than the head and, as a result, two shock waves originate during regeneration of the desiccant. In this case, the state properties of the air stream and the desiccant vary discontinuously in time and space and the method of characteristics is not applicable.

To calculate the speed of the shocks and the properties of the state between the two shocks, a generalized shock wave theory is applied as proposed by Lax [22]. The state between the two shocks is defined as the shock state and referred to by the subscript 's'. Conservation of mass and energy across a shock is expressed as a jump condition [2]. The jump condition for the first shock may be written as the following matrix equation:

$$\begin{bmatrix} w_s - w_{11} \\ i_s - i_{11} \end{bmatrix} = S_1 \begin{bmatrix} W_s - W_{11} \\ I_s - I_{11} \end{bmatrix} \tag{12a}$$

and for the second shock:

$$\begin{bmatrix} w_{21} - w_s \\ i_{21} - i_s \end{bmatrix} = S_2 \begin{bmatrix} W_{21} - W_s \\ I_{21} - I_s \end{bmatrix}. \tag{12b}$$

S_i is the speed of the ith shock in the dimensionless coordinate system (x, τ). S_1 and S_2 may be eliminated from equations (12) and the following expressions are obtained:

$$\begin{aligned} (w_s - w_{11})(I_s - I_{11}) &= (W_s - W_{11})(i_s - i_{11}) \\ (w_{21} - w_s)(I_{21} - I_s) &= (W_{21} - W_s)(i_{21} - i_s). \end{aligned} \tag{13}$$

Equations (13) must be solved numerically in combination with the state property relationships (4) to provide the shock state properties (t_s, w_s) for given process and regneration air inlet states. For the hyperbolic system (7), these equations have two distinct solutions [24] of which only one is physically possible. This solution satisfies the jump condition (12) and also the following entropy condition [22]:

$$\begin{aligned} \lambda_{1,11} < S_1 < \lambda_{1,s} \\ \lambda_{2,s} < S_2 < \lambda_{2,21}. \end{aligned} \tag{14}$$

S_1 and S_2 may be obtained from equations (12) after solving (13).

4. ROTARY DEHUMIDIFIER OPERATING CHART

Figure 6 shows a typical combined characteristic or wave diagram for a counterflow ideal dehumidifier in a periodic steady state. The F_1 and F_2 rarefaction waves during the processing period (i.e. period 1) are

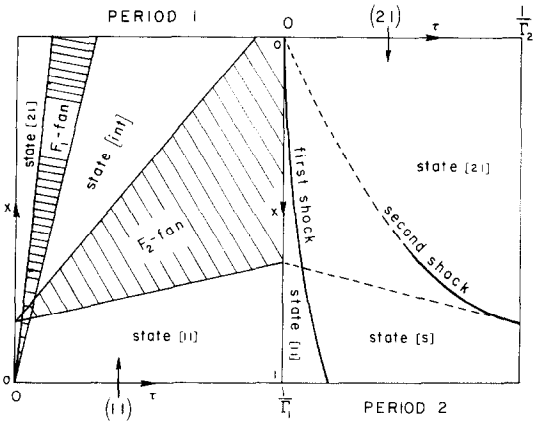

FIG. 6. Wave diagram for the ideal rotary heat and mass exchanger.

illustrated by two separated fans of characteristics in a τ–x coordinate system. The state properties of process air stream and desiccant are constant outside the two conical areas covered by the fans, while varying continuously inside those areas. The two shocks during the regeneration period (i.e. period 2) are also illustrated in Fig. 6. The first shock originates from the regeneration-period entrance face of the dehumidifier wheel. The second shock evolves slowly by contraction of the F_2 wave (dotted lines in Fig. 6) and is fully developed at the end of period 2 (solid line). The state in front of the second shock is the shock state 's'. The distance that the various waves move through the desiccant depends on the velocity of the wave, λ_i, or S_i, which is a function of both inlet states, and on the duration of each period, $1/\Gamma_j$.

Only the F_1 wave and the first shock pass completely through the matrix for each revolution in this illustration. The F_2 wave and the second shock do not reach the exit face of the dehumidifier. If the trailing edge of the F_2 rarefaction wave were to reach the exit face of the desiccant wheel during the processing period, the desiccant would be in complete equilibrium with the process air inlet state before the matrix enters the regeneration period. Similarly, if the second shock were to propagate completely through the matrix during the regeneration period, the desiccant would be in complete equilibrium with the regeneration air inlet state before entering the processing period.

These ideas lead to the concept of an operating chart for rotary heat and mass exchangers, as shown in Fig. 7. This figure illustrates the alternate modes of dehumidifier operation on a Γ_1-Γ_2 capacitance rate diagram. The solid line A–B–D represents the dehumidifier regeneration line. The area to the right of the regeneration line in the chart is the region of complete regeneration. If the dehumidifier were to be operated at an operating point (Γ_1, Γ_2) within the region of complete regeneration (e.g. points 1–3 in Fig. 7), the second shock would move completely through the matrix during the regeneration period. All of the

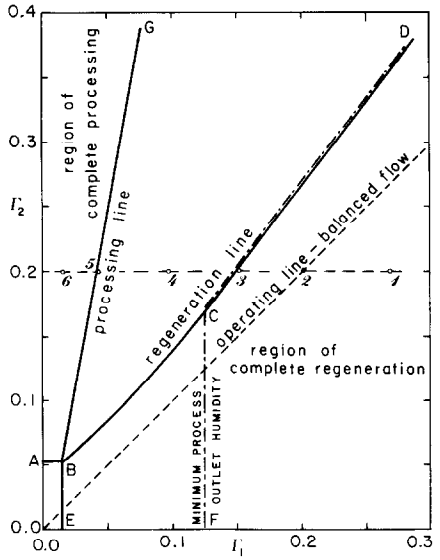

FIG. 7. Operating chart for the ideal rotary heat and mass exchanger. Inlet conditions 25.0°C, 15.0 g kg^{-1} and 85.0°C, 15.0 g kg^{-1}.

desiccant particles would then be in complete equilibrium with the regeneration air inlet state before they enter period 1. Point 2 in Fig. 7 is located on the operating line for balanced flow. Process and regeneration air flow rates are equal for the balanced flow-operating line, which is situated inside the region of complete regeneration. Because of the nonlinearity of the desiccant–fluid property relationships (4), the capacity of the hot air stream to dry the desiccant is higher than the capacity of the desiccant to dry the cold air stream at equal flow rates. Point 3 in Fig. 7 is located on the regeneration line. For this operating point, the second shock just reaches the exit face of the wheel during regeneration.

The solid line E–B–D in Fig. 7 represents the dehumidifier processing line. The area to the left of the processing line is the region of complete processing. If the dehumidifier were to be operated at an operating point (Γ_1, Γ_2) within the region of complete processing (e.g. points 5 and 6 in Fig. 7), the trailing edge of the the F_2 wave would move completely through the matrix during the processing period. Thus, all the desiccant particles would reach equilibrium with the process air inlet state during the processing period before they enter period 2. This is the case for low values for Γ_1, or high process air flow rates. Point 5 in Fig. 7 is located on the processing line. For this operating point, the trailing edge of the F_2 wave just reaches the exit face of the wheel during the processing period.

For intermediate values of Γ_1 (e.g. point 4 in Fig. 7), dessicant particles located at the exit face of the dehumidifier wheel never reach complete equilibrium with either the process or regeneration air inlet states. A complex interaction of shocks and rarefaction waves occurs as illustrated in the wave diagram, Fig. 6.

The regeneration line has a positive slope. If more air is being processed for a given rotational speed, then more air is required to completely regenerate the desiccant matrix. Similarly, the processing line has a positive slope. Correlations for regeneration and processing lines are given in the next section. The region of complete processing and complete regeneration overlap in the square 0.0–A–B–E in Fig. 7. The line segment A–B is a straight line with zero slope because it lies in the region of complete processing:

$$\Gamma_{2,A} = \Gamma_{2,B} = S_2 \tag{15a}$$

where S_2 is the speed of the second shock when regenerating a fully processed desiccant. The line segment E–B is a straight line with infinite slope. The following equation holds:

$$\Gamma_{1,E} = \Gamma_{1,B} = \lambda_{2,11}. \tag{15b}$$

The performance correlations that are listed in the next section may be used to show that the process air mean outlet humidity ratio is a minimum for certain values of Γ_1 and Γ_2 [24]. The dashed line F–C–D in Fig. 7 represents this minimum. This minimum value is constant for the segment F–C but increases slowly along the line C–D as Γ_1 increases. The line F–C is a straight line with infinite slope because the segment lies in the region of complete regeneration of the desiccant and is not dependent on Γ_2. Outside the region of complete regeneration, the line of minimum outlet humidity ratio coincides with the regeneration line of the dehumidifier.

5. PERFORMANCE CORRELATIONS

The method of characteristics and the shock wave method provide a set of analytical equations that allow prediction of the performance of an ideal dehumidifier for the entire range of capacitance parameters, and for any inlet conditions. These performance correlations are valid for either the region of complete regeneration or the region of complete processing. Correlations for the processing line and the regeneration line are provided.

The solution to the coupled conservation equations (7) and initial (5) and boundary conditions (6) consists of determining the mean outlet state of one of the two fluid streams:

$$\bar{w}_{j2} = \Gamma_j \int_0^{1/\Gamma_j} w_m(x = 1, \tau)_j \, d\tau$$
$$\bar{i}_{j2} = \Gamma_j \int_0^{1/\Gamma_j} i_m(x = 1, \tau)_j \, d\tau \tag{16}$$

where $w_m(x, \tau)_j$ amd $i_m(x, \tau)_j$ are the solutions to equations (4)–(7) for period j of the regenerator. The outlet state of the other fluid stream may then be obtained by applying an overall mass and energy

balance to the dehumidifier:

$$\frac{(w_{11}-\bar{w}_{12})}{\Gamma_1}=\frac{(\bar{w}_{22}-w_{21})}{\Gamma_2}$$
$$\frac{(i_{11}-\bar{i}_{12})}{\Gamma_2}=\frac{(\bar{i}_{22}-i_{21})}{\Gamma_2}. \tag{17}$$

The process air outlet state as a function of time for the region of complete regeneration may be obtained by the method of characteristics [24]. The shock wave method provides the regeneration air outlet state as a function of time for the region of complete processing [24]. Table 1 lists fluid stream outlet states as functions of time for both modes of operation. Integration (16) may now be carried out analytically (for those time-intervals where the fluid outlet state is constant) or numerically for the other intervals.

Analytical expressions for regeneration line and processing line are derived in Appendices A and B, respectively, and are given by

$$\Gamma_{2,R}=\Gamma_1\frac{(w_s-w_{21})}{(w_{11}-w_{int})+\Gamma_1\left(\frac{w_s-w_{11}}{S_1}-\frac{w_{21}-w_{int}}{\bar{\lambda}_1}\right)}, \tag{18a}$$

where $\bar{\lambda}_1$ is defined as

$$\frac{1}{\bar{\lambda}_1}=\frac{0.5}{\lambda_{1,21}}+\frac{0.5}{\lambda_{1,int}}, \tag{18b}$$

and by

$$\Gamma_{1,p}=\frac{\lambda_{2,11}}{1-\left(1-\frac{S_2}{\Gamma_2}\right)\left(\frac{\bar{\lambda}_1-\lambda_{2,11}}{\bar{\lambda}_1-\lambda_{2,s}}\right)}, \tag{19a}$$

and where $\bar{\lambda}_1$ is defined by:

$$\bar{\lambda}_1=\frac{\lambda_{1,11}+\lambda_{1,s}}{2}. \tag{19b}$$

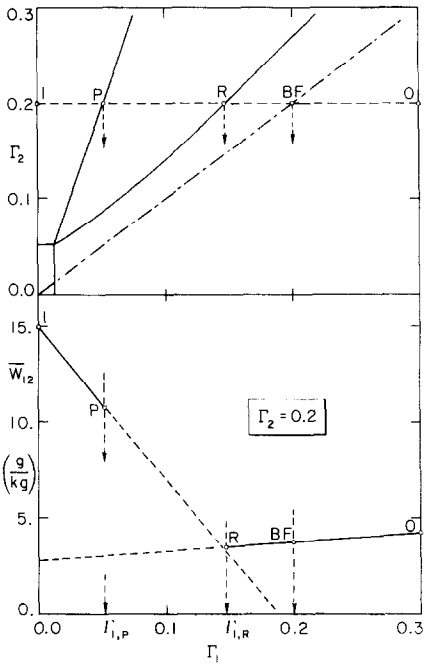

FIG. 8. Process air outlet humidity ratio as a function of capacitance parameter Γ_1. Inlet conditions 25.0°C, 15.0 g kg^{-1} and 85.0°C, 15.0 g kg^{-1}.

Integration of equation (16) may be carried out for a silica gel dehumidifier with specified inlet conditions [24]. An illustration of such an integration is graphically shown in Fig. 8. The mean humidity ratio of the process air outlet state, $\bar{w}_{12}$, as a function of Γ_1 is illustrated in this figure. The solid line R–O in Fig. 8 is obtained from the integration (16) of the expression for $w_{12}(\tau)$ as listed in Table 1. This expression is valid only for the region of complete regeneration:

$$\Gamma_1 \geqslant \Gamma_{1,R}. \tag{20}$$

Table 1. Fluid stream outlet state as a function of time

Process air outlet state for the region of complete regeneration

$$\Gamma_2 \leqslant \Gamma_{2,R}(t_{11}, w_{11}, t_{21}, w_{21}, \Gamma_1)$$

for τ:	$0 \leqslant \tau \leqslant \frac{1}{\lambda_{1,21}}$	$\frac{1}{\lambda_{1,21}} \leqslant \tau \leqslant \frac{1}{\lambda_{1,int}}$	$\frac{1}{\lambda_{1,int}} \leqslant \tau \leqslant \frac{1}{\lambda_{2,int}}$	$\frac{1}{\lambda_{2,int}} \leqslant \tau \leqslant \frac{1}{\lambda_{2,11}}$	$\frac{1}{\lambda_{2,11}} \leqslant \tau$
$w_{12}(\tau)=$	w_{21}	$w_m(\lambda_1=1/\tau, F_2=F_{2,21})$	w_{int}	$w_m(\lambda_2=1/\tau, F_1=F_{1,11})$	w_{11}
$i_{12}(\tau)=$	i_{21}	$i_m(\lambda_1=1/\tau, F_2=F_{2,21})$	i_{int}	$i_m(\lambda_2=1/\tau, F_1=F_{1,11})$	i_{11}

Regeneration air outlet state for the region of complete processing

$$\Gamma_1 \leqslant \Gamma_{1,P}(t_{11}, w_{11}, t_{21}, w_{21}, \Gamma_2)$$

for τ:	$0 \leqslant \tau \leqslant \frac{1}{S_1}$	$\frac{1}{S_1} \leqslant \tau \leqslant \frac{1}{S_2}$	$\frac{1}{S_2} \leqslant \tau$
$w_{22}(\tau)=$	w_{11}	w_s	w_{21}
$i_{22}(\tau)=$	i_{11}	i_s	i_{21}

$\Gamma_{1,R}$ is obtained from (18) for the regeneration line of the dehumidifier, for specified inlet conditions and Γ_2. Point BF in Fig. 8 illustrates the operating point for balanced flow.

The solid line I–P in Fig. 8 is obtained from the integration (16) of the expression for $w_{22}(\tau)$ (Table 1), and applying the overall mass balance (17). The expression for $w_{22}(\tau)$ is valid only for the region of complete processing:

$$\Gamma_1 \leqslant \Gamma_{1,P}, \tag{21}$$

where $\Gamma_{1,P}$ is obtained from (19). For intermediate values of Γ_1, no correlation is available because of the complex interaction between the two wave phenomena in both periods. However, negligible errors are introduced if points P and R are connected by a parabola. $\bar{w}_{12}(\Gamma_1)$ and $\bar{i}_{12}(\Gamma_1)$ are continuous curves with continuous first derivatives at point P and discontinuous first derivatives point R, because of the shock waves during the regeneration period.

6. COMPARISON WITH EXISTING SOLUTION METHODS

To predict the performance of a dehumidifier with finite transfer coefficients, a general computer code, MOSHMX, has been developed by Maclaine-cross [14] that solves equation (3) with the initial conditions (5) and the boundary conditions (6). The program is based on a second-order finite-difference method with extrapolation to zero grid size. This computer program was used to compare the proposed correlations given by equation (16) and Table 1 with performance values provided by that program. In the limit:

$$\begin{aligned} NTU_{t,j} &\to \infty \\ NTU_{w,j} &\to \infty \end{aligned} \tag{22}$$

the real dehumidifier performance approaches that of an ideal dehumidifier. Fig. 9 shows $\bar{w}_{12}$ as a function of Γ_1 for a fixed value of Γ_2 and various values of $NTU_{t,j}$. The convergence to the proposed correlation is clearly shown. Further comparisons are given in ref. [24].

7. CONCLUSIONS

The governing mass and energy conservation equations for a dehumidifier with infinite transfer coefficients are analyzed using the method of characteristics and the shock wave method. The method of characteristics is applicable when the desiccant is processing the low temperature air stream. The shock wave method is applicable when the desiccant is being regenerated by the high temperature air stream. Depending on the operating parameters, Γ_1 and Γ_2, the performance of the ideal dehumidifier is determined either by the propagation of two expansion waves during the processing period or by the propagation of two shock waves during the regeneration period.

A dehumidifier operating chart is introduced in the form of a Γ_1-Γ_2 diagram which shows these two regions. In each region, either the shock wave method or the method of characteristics provides analytical performance correlations. The process air outlet state of the ideal dehumidifier calculated using these correlations is in good agreement with that obtained from a finite-difference computer program for a dehumidifier with high heat and mass transfer coefficients. No assumptions are made with respect to the desiccant or the fluid state properties. Therefore, the analysis may be applied to other desiccants such as molecular sieves, manganese dioxide or lithium chloride.

In part II of this paper, correlations for the

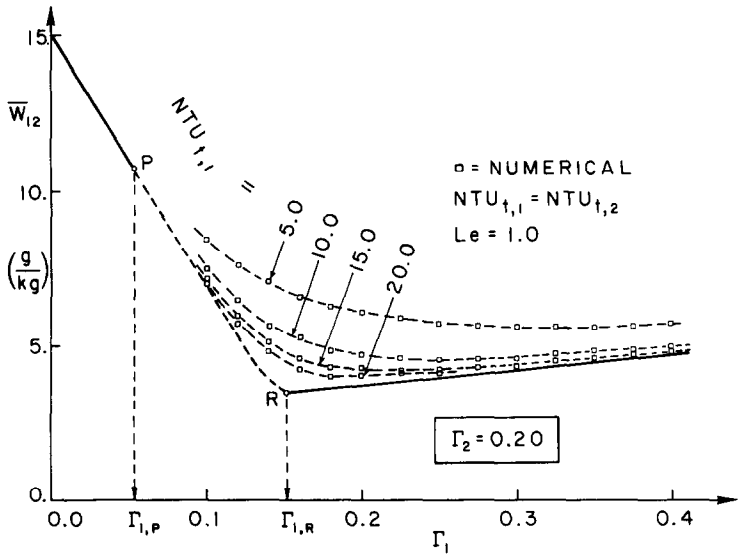

FIG. 9. Comparison of humidity ratio correlations with the finite-difference solution from ref. (14).

effectiveness of dehumidifiers with finite transfer coefficients are given as functions of the number of transfer units.

Acknowledgement—This project was supported by the Solar Heating and Cooling Research and Development Branch, Office of Conservation and Solar Applications, U.S. Department of Energy.

REFERENCES

1. B. Palancz, Analysis of solar-dehumidification drying, *Int. J. Heat Mass Transfer* **27**, 647–655 (1984).
2. S. Matsumoto and D. C. T. Pei, A mathematical analysis of pneumatic drying of grains, *Int. J. Heat Mass Transfer* **27**, 843–849, 851–855 (1984).
3. N. J. Macdonald, Utilization of condenser heat for desiccant dehumidifiers in supermarket applications, *Trans. Am. Soc. Heat. Refrig. Air-Condit. Engrs* **89**, 225–235 (1983).
4. J. E. Clark, A. F. Mills and H. Buchberg, Design and testing of thin adiabatic desiccant beds for solar air conditioning applications, *J. sol. Energy Engng* **103**, 89–91 (1981).
5. D. Gidaspow, Z. Lavan, M. Onischak and S. Perkari, Development of solar desiccant dehumidifier, *Proc. 13th Intersociety Energy Confersion Engineering Conferences*, pp. 1623–1627 (1978).
6. J. Rousseau, Development of a solar desiccant dehumidifier, Rep. 81-18436, AiResearch Manufacturing Company, Los Angeles (1981).
7. B. Huskey, J. Sharp, A. Venero and H. Yen, Advanced solar/gas desiccant cooling system, Rep. 81/0064, Gas Research Institute, Chicago (1982).
8. D. Schlepp, A high performance dehumidifier for solar desiccant cooling systems, Rep. TP-252-1979, Solar Energy Research Institute, Denver (1983).
9. R. A. Macriss and T. S. Zawacki, High CDP rotating wheel solid desiccant system, *Proc. 9th Energy Technology Conference*, Washington, D.C. (1982).
10. R. V. Dunkle, A method of solar air conditioning, *Mech. Chem. Engng Trans. Instn Engrs Aust.* **1**, 73–78 (1965).
11. P. J. Banks, Coupled equilibrium heat and single adsorbatc transfer in fluid flow through a porous medium—I. Characteristic potentials and specific capacity ratios, *Chem. Engng Sci.* **27**, 1143–1156 (1972).
12. D. J. Close and P. J. Banks, Coupled equilibrium heat and single adsorbate transfer in fluid flow through a porous medium—II. Predictions for a silica-gel-air-drier using characteristic charts, *Chem. Engng Sci.* **27**, 1157–1169 (1972).
13. I. L. Maclaine-cross and P. J. Banks, Coupled heat and mass transfer in regenerators—prediction using an analogy with heat transfer, *Int. J. Heat Mass Transfer* **15**, 1225–1242 (1972).
14. I. L. Maclaine-cross, A theory of combined heat and mass transfer in regenerators. Ph.D. thesis, Monash University, Australia (1974).
15. J. J. Jurinak and P. J. Banks, A numerical evaluation of two analogy solutions for a rotary silica gel dehumidifier. In *Heat Transfer in Porous Media* (edited by J. V. Beck and L. S. Yao), HTD 22, pp. 57–68, American Society of Mechanical Engineers, New York (1982).
16. R. K. Shah, Thermal design theory for regenerators. In *Heat Exchangers: Thermal–Hydraulic Fundamentals and Design* (edited by S. Kakac, A. E. Bergles and F. Mayinger), pp. 721–763. Hemisphere, New York (1981).
17. B. Mathiprakasam and Z. Lavan, Performance predictions for adiabatic desiccant dehumidifiers using linear solutions, *J. sol. Energy Engng* **102**, 73–79 (1980).
18. C. E. Bullock and J. L. Threlkeld, Dehumidification of moist air by adiabatic adsorption, *Trans. Am. Soc. Heat. Refrig. Air-Condit. Engrs* **72**, 301–313 (1966).
19. D. Roy and D. Gidaspow, A cross flow regenerator—a Green's matrix representation, *Chem. Engng Sci.* **27**, 779–793 (1972).
20. J. B. Ingram and G. C. Vliet, Solid desiccant rotary dryer performance charts, *Prog. sol. Energy* **5**, 603–608 (1982).
21. J. J. Jurinak, Open cycle desiccant cooling-component models and systems simulations. Ph.D. thesis, University of Wisconsin—Madison (1982).
22. P. Lax, *Hyperbolic Systems of Conservation Laws and the Mathematical Theory of Shock Waves*. SIAM, Philadelphia (1973).
23. I. S. Berezin and N. P. Zhidkov, *Computing Methods*. Addison Wesley, Massachusetts (1965).
24. E. Van den Bulck, Analysis of solid desiccant rotary dehumidifiers. M.S. thesis, University of Wisconsin—Madison (1983).
25. A. J. Chorin, Random choice solution of hyperbolic systems, *J. comput. Phys.* **22**, 517–533 (1976).
26. E. Van den Bulck, J. W. Mitchell and S. A. Klein, The design of dehumidifiers for use in desiccant cooling and dehumidification systems, ASME Paper No. 84-HT-32, 22nd ASME–AIChE National Heat Transfer Conference, Niagara Falls (1984).

APPENDIX A: CORRELATION FOR REGENERATION LINE

The following assumptions are made to obtain the expression for the regeneration line:

(1) The second shock wave is fully developed during the regeneration period. The continuous F_2 wave is completely converted into a strong shock.
(2) The leading edge of the F_2 rarefaction wave has not reached the regenerating inlet face of the matrix during the processing period.

Assumption 1 has been verified by solving (7) and the following initial value problem:

at $\tau = 0$,

$$\begin{aligned} t(x,\tau) &= t_{\text{int}}; \quad \text{for} \quad x = 0 \\ w(x,\tau) &= w_{\text{int}} \\ F_1(t,w) &= F_{1,11}; \quad \text{for} \quad \text{all } x,\ 0 \leqslant x \leqslant x_0 \\ \lambda_2(t,w) &= (1-x)\Gamma_1 \\ t(x,\tau) &= t_{11}; \quad \text{for} \quad \text{all } x,\ x_0 \leqslant x \leqslant 1 \\ w(x,\tau) &= w_{11} \end{aligned} \tag{A1}$$

at $x = 0$,

$$\begin{aligned} t(x,\tau) &= t_{21}; \quad \text{for all} \quad \tau > 0 \\ w(x,\tau) w_{21} & \end{aligned}$$

by a numerical scheme, analogous to Glimm's sampling procedure [25] that has been developed to solve shock wave problems. Equations (7) and (A1) were solved for a number of operating parameters and inlet conditions. Assumption 2 may be expressed as

$$\Gamma_1 \geqslant \lambda_{2,1\text{-int}}. \tag{A2}$$

This assumption is closely met for most operating points for well-defined dehumidifiers [26].

The outlet humidity ratio of the regeneration air stream is then given by integration of equation (16):

$$\bar{w}_{22} = \Gamma_{2,R}\left[\frac{w_{11}}{\bar{S}_1} + w_s\left(\frac{1}{\Gamma_{2,R}} - \frac{1}{\bar{S}_1}\right)\right] \tag{A3}$$

$\bar{S}_1$ denotes the average speed of the first shock. The overall mass balance (17) may be substituted in (A3) to yield the following expressions for $\Gamma_{2,R}$:

$$\Gamma_{2,R} = \Gamma_1 \frac{(w_s - w_{21})}{(w_{11} - \bar{w}_{12}) + \frac{\Gamma_1}{\bar{S}_1}(w_s - w_{11})}. \quad \text{(A4)}$$

The mean humidity ratio of the process air outlet state may be expressed by integration of equation (16):

$$\bar{w}_{12} = w_{int} + \frac{\Gamma_1}{\bar{\lambda}_1}(w_{21} - w_{int}) \quad \text{(A5)}$$

where $\bar{\lambda}_1$ is the average speed of the F_1 rarefaction wave. Substituting (A5) in (A4) yields

$$\Gamma_{2,R} = \Gamma_1 \frac{(w_s - w_{21})}{(w_{11} - w_{int}) + \Gamma_1\left(\frac{w_s - w_{11}}{\bar{S}_1} - \frac{w_{21} - w_{int}}{\bar{\lambda}_1}\right)} \quad \text{(A6)}$$

which is equivalent to equation (18).

Accurate values for $\bar{S}_1$ and $\bar{\lambda}_1$ are not needed. Numerical evaluations of expression (A6) shows that the second term of the denominator represents a correction term. $\bar{\lambda}_1$ and $\bar{S}_1$ may be calculated by

$$\bar{S}_1 = S_1$$
$$\frac{1}{\bar{\lambda}_1} = \frac{0.5}{\lambda_{1,21}} + \frac{0.5}{\lambda_{1,int}} \quad \text{(A7)}$$

APPENDIX B:

CORRELATION FOR PROCESSING LINE

The correlation for the processing line may be obtained by analyzing the following initial value problem:

$$\begin{aligned}
&\text{at } \tau = 0, \quad t(x,\tau) = t_s; \quad \text{for all } x,\ 0 \leqslant x \leqslant x_0 \\
&\qquad w(x,\tau) = w_s \\
&\qquad t(x,\tau) = t_{21}; \quad \text{for all } x,\ x_0 \leqslant x \leqslant 1 \\
&\qquad w(x,\tau) = w_{21} \\
&\text{at } x = 0, \quad t(x,\tau) = t_{11}; \quad \text{for all } \tau > 0 \\
&\qquad w(x,\tau) = w_{11}.
\end{aligned} \quad \text{(B1)}$$

The solution to the Riemann problem (7) and (B1) is illustrated in Fig. A1. The characteristics originating from the x-axis are shown in the x–τ plane. During the regeneration period, the second shock has partially moved through the processed desiccant:

$$x_0 = 1 - \frac{S_2}{\Gamma_2}. \quad \text{(B2)}$$

The trailing edge of the F_2 wave travels at a speed $\lambda_{2,s}$ for a time τ_0 given by

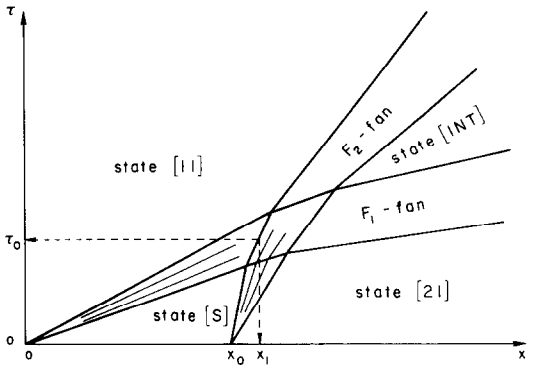

FIG. A1. Characteristic diagram for processing a partially regenerated desiccant matrix.

$$x_0 + \lambda_{2,s}\tau_0 = \bar{\lambda}_1\tau_0, \quad \text{(B3)}$$

where $\bar{\lambda}_1$ is the average speed of the F_1 wave:

$$\bar{\lambda}_1 = \frac{\lambda_{1,11} + \lambda_{1,s}}{2}. \quad \text{(B4)}$$

The distance traveled by the trailing edge of the F_2 wave, x_1, is then given by

$$x_1 = \bar{\lambda}_1\tau_0 = \frac{\bar{\lambda}_1 x_0}{\bar{\lambda}_1 - \lambda_{2,s}}. \quad \text{(B5)}$$

The time needed to complete the remainder of the path, $1 - x_1$, at a speed $\lambda_{2,11}$ is given by

$$\tau_1 = \frac{1 - x_1}{\lambda_{2,11}}. \quad \text{(B6)}$$

Substituting (B5) into (B6) yields

$$\tau_1 = \frac{1}{\lambda_{2,11}} - \frac{\bar{\lambda}_1}{\lambda_{2,11}} \frac{x_0}{\bar{\lambda}_1 - \lambda_{2,s}}. \quad \text{(B7)}$$

The total time, τ, that is needed for the trailing edge of the F_2 wave to reach the exit face of the regenerator is then given by:

$$\tau = \tau_0 + \tau_1. \quad \text{(B8)}$$

Solving (B3) and substituting (B2), (B6) into (B7) yields

$$\tau = \frac{1}{\lambda_{2,11}} - \frac{\left(1 - \frac{S_2}{\tau_2}\right)}{\lambda_{2,11}}\left(\frac{\bar{\lambda}_1 - \lambda_{2,11}}{\bar{\lambda}_1 - \lambda_{2,s}}\right). \quad \text{(B9)}$$

The expression for the processing line, equation (19), may then be obtained from

$$\Gamma_{1,P} = \frac{1}{\tau}. \quad \text{(B10)}$$

THEORIE DE DIMENSIONNEMENT DES ECHANGEURS ROTATIFS DE CHALEUR ET DE MASSE—I. ANALYSE ONDULATOIRE DES EXCHANGEURS ROTATIFS AVEC DES COEFFICIENTS DE TRANSFERT INFINIS

Résumé—On présente une théorie pour modéliser des échangeurs rotatifs de chaleur et de masse avec des coefficients de transfert infinis. Les équations de continuité et d'énergie, pour un écoulement monodimensionnel transitoire sont établies et analysées. Des solutions sont obtenues par la méthode des caractéristiques et par la méthode de l'onde de choc. Les deux méthodes fournissent un système d'équations analytiques qui fournissent les estimations de performance de l'échangeur de chaleur et de masse avec des coefficients infinis de transfert pour des conditions opératoires. Un graphe est présenté qui montre les modes fondamentaux de fonctionnement pour les échangeurs rotatifs de chaleur et de masse. La partie II présentera des formules pour l'efficacité des deshumidificateurs tournants avec des coefficients de transfert finis.

AUSLEGUNGSTHEORIE FÜR ROTIERENDE WÄRME- UND STOFFAUSTAUSCHER—TEIL I. WELLENANALYSE VON ROTIERENDEN WÄRME- UND STOFFAUSTAUSCHERN MIT UNENDLICHEN TRANSPORTKOEFFIZIENTEN

Zusammenfassung—Es wird eine Theorie zur Modellierung von Wärme- und Stoffaustauschern mit unendlich großen Transportkoeffizienten vorgestellt. Die Kontinuitäts- und Energiegleichung für die eindimensionale instationäre Strömung werden aufgestellt und untersucht. Lösungen für die Gleichungen werden mit Hilfe des Charakteristiken-Verfahrens und der Stoßwellenmethode ermittelt. Beide Methoden liefern einen Satz analytischer Gleichungen, die eine Vorhersage der Güte eines Wärme- und Stoffübertragers mit unendlich großen Transportkoeffizienten für alle Eintritts- und Betriebsbedingungen erlauben. Ein Kennlinienblatt für Regeneratoren wird vorgestellt, das die grundlegenden Betriebsarten von rotierenden Wärme- und Stoffübertragern zeigt. Teil II gibt Beziehungen für die Wirksamkeit von rotierenden Trocknern mit endlichen Transportkoeffizienten an.

ТЕОРИЯ ВРАЩАЮЩИХСЯ ТЕПЛОМАССООБМЕННИКОВ. I. ВОЛНОВНОЙ АНАЛИЗ ВРАЩАЮЩИХСЯ ТЕПЛОМАССООБМЕННИКОВ ПРИ БЕСКОНЕЧНЫХ КОЭФФИЦИЕНТАХ ПЕРЕНОСА

Аннотация—Представлена теория моделирования вращающихся тепло-и массообменников при бесконечных коэффициентах переноса. Для одномерного неустановившегося течения получены и проанализированы уравнения неразрывности и энергии. Рашения уравнений получены методом характеристик и ударно-волновым методом. Оба метода представляют систему аналитических уравнений, позволяющих проводить расчет тепло-и массообменника с бесконечными коэффициентами переноса для любых начальных рабочих условий. Представлена схема работы регенератора, которая выделяет основные режимы работы вращающихся тепло-и массообменников. Во второй части представлены зависимости для эффективностей осушителей с конечными коэффициентами переноса.